Update on Fast Ignition Experiments at Nova Petawatt

R.B. Stephens,[1] T.E. Cowan,[2*] R.R. Freeman,[3] S.P. Hatchett,[2] M.H. Key,[2] J.A. Koch,[2] R.W. Lee,[2] A. MacKinnon,[2] D. Pennington,[2] R. Snavely,[3] M. Tabak,[2] and K. Yasuike[2]

[1]General Atomics, P.O. Box 85608, San Diego, California 92186-5608
email: stephens@fusion.gat.com
[2]Lawrence Livermore National Laboratory, P.O. Box 808, Livermore, California 94550
[3]UC Davis, Livermore, California
[*]Current address General Atomics

Abstract. The physics of fast ignition was studied on the PetaWatt laser facility at LLNL for ~3 years, to May 1999. The previous report to this conference described experiments that demonstrated the efficient transfer of laser energy to relativistic electrons that penetrated into the target and heated to temperatures ~1 keV. Since then, we have looked at energy transfer and propagation in dense plasmas in considerably more detail. Measurements show that the relativistic electrons penetrate >100 µm into a CH foil in a collimated beam with a complex annular structure. Production of an energetic (up to 55 MeV) proton beam was also discovered. The protons are tightly bunched (<40° spread) and are emitted normal to the back target surface, so can be accurately directed. This gives another promising possibility for delivery of the ignition pulse.

1. Introduction

The PetaWatt laser (PW) in the Nova facility at LLNL was in operation for ~3 years, to May 1999. It could deliver 500 J in 20 to 0.5 ps at 10^{19} to 3×10^{20} W/cm^2 into a spot ~10 µm across, with much smaller prepulses (fractional powers of 1.5×10^{-5} amplified spontaneous emission and 3×10^{-4} leakage). In this regime, the EM fields drive electrons to relativistic energies with intensities suitable for target ignition in the Fast Ignitor concept. At the last IAEA Conference on Fusion Energy, we reported on initial results from the PW laser relevant to fast ignition and showed the potential of fast ignition to give a gain of 300× using the NIF laser as driver [1]. New diagnostics have been added since that report and the energy transport investigated further. The physics of energy transport appears to be much richer than previously supposed. The electron current was found to exhibit a surprisingly complex structure which was apparently invariant to substantial depths (Section 2). In addition, a tightly focussed beam of protons was discovered (Section 3); it had been observed and noted in the previous paper, but was then thought to be electrons. These protons allow a new option for delivering the ignition pulse.

2. Electron propagation

The laser pulse generates ~ 100 MA relativistic electron beam. This is much larger than the Alvèn limit, so the initial jet of electrons is subject to filamentation by the Weibel instability. A strong quasi-static magnetic field tends to compress these current filaments, but that effect is modified by the return current sheath around each filament. All these processes affect the deep heating of solid matter by laser-generated electrons. They have been simulated [2], but the problem, combining both high particle densities and long times and long distances (relative to a light wave), is currently beyond the reach of first principles modeling, and experimental data is needed to guide research.

Earlier experiments investigated heating near the surface [3]. Our experiments used x-ray emissions from thin metal layers (Al, Au) buried in the lower CH matrix to examine the propagation of electron beams up to 200 µm from the laser impact spot, and away from the disturbing influence of plasma surfaces. Their emission spectra show the temperature and pinhole images show the distribution [4,5].

Three diagnostics viewed the x-ray emission from the Al or Au tracer layers. The first was a pinhole camera, with a filtered array of 10 µm pinholes in a Ta substrate projecting images onto film or an x-ray charge-coupled device (CCD). The camera imaged the front or the back of the target, depending on the experiment (foils more than 30 µm from the front surface were

5 μm from the back surface, and could be viewed from the back with minimal matrix absorption), with a spatial resolution of ~10 μm for x-ray energies > 1.5 keV. The second diagnostic was a concave-spherical mica crystal spectrograph [6], which delivered a spectral resolution $\Delta E/E < 2.5\times10^{-3}$ onto an x-ray CCD. The third diagnostic was a convex-cylindrical potassium-hydrogen-phthalate (KAP) crystal spectrograph, which delivered a spectral resolution $\Delta E/E < 5\times10^{-3}$ onto a streak camera with a time resolution of 25–80 ps depending on the experiment. The spectrographs were operated on front-view Al-tracer experiments only.

The pinhole images show evidence of deep, collimated penetration of the electron beam. Representative x-ray images are shown in Fig. 1. Front view Al layers 10–25 μm deep [Fig. 1(a)] showed annular images with 70–120 μm inner diameters (compared to a beam spot size ~10 μm) Front view Al layers 30–50 μm deep [Fig. 1(b)] showed ~50 μm regions of arc-like structure, possibly due to weaker signals which permitted only the brightest portions of the rings to be observed. Rear view Au layers 50–100 μm from the front surface (buried ~5 μm under the back surface) [Fig. 1(c)] showed rings ~50 μm in diameter. We also obtained a rear-view image from an Au tracer 200 μm deep, but the exposure was too weak to exhibit structure. In comparison, the images from solid Al and Au targets (front view) [Fig. 1(d)] were sub 20 μm dots.

Spectroscopic data confirm that the rings are emitted from the buried metal tracers, since Al tracer targets show emission lines from highly ionized Al (Fig. 2). The integrated exposures of the spectra and the pinhole images are strongly correlated, indicating that the spectra are emitted from the bright regions of the images. In addition, time-resolved spectra indicate that all keV x-ray emission takes place with a half-maximum duration ~70 ps (*e.g.* it lasts much longer than the 5 ps laser pulse), indicating thermal emission.

The spectra also indicate the bulk electron temperature, T_e in the buried films. The measured Al XII line ratio $(2p^{2\,1}D_2\text{-}1s2p\,^1P_1)/(1s3p\text{-}1s^2)$, He-J/He-β, is fitted with a simulation of local thermodynamic equilibrium (LTE) optically-thin spectra using the code TOTAL. A representative spectrum with a TOTAL fit is shown in Fig. 2(a).

Self-consistent time-integrated T_e and mass density (ρ) data for Al at 5–30 μm depths, show T_2 ~300 eV and ρ = 0.25–0.95 g/cm^3. We do not observe any systematic dependence of T_e or ρ on layer depth, suggesting nearly isothermal heating at constant density.

3. Proton beams

A last-minute addition to the previous IAEA presentation [1] was observation on radiographic film of a highly collimated energetic beam coming from the back of the target. At that time the beam was thought to be a beam of electrons generated by the laser-plasma interaction at the front of the foil. Analysis of etched tracks in filtered CR-39 plastic gave evidence that it was in fact composed of > 30 MeV protons. Re-analysis of that film data gave a plausible energy content of 10 J (~7% of the energy in the incident laser beam) and a source temperature of ~4 MeV. Subsequent experiments added more detail.

The radiochromic film data in Fig. 3 shows an intense proton beam emitted normal to the target surfaces. The angular spread of this beam has a sharp cut-off which depends on energy;

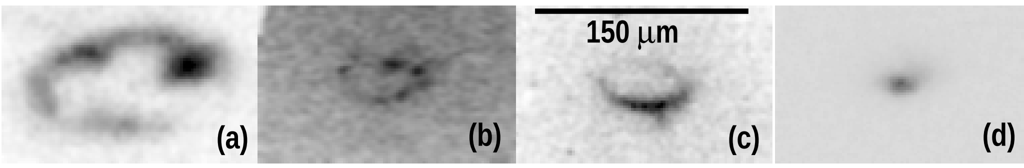

FIG. 1. X-ray pinhole images of thin diagnostic layers buried in CH targets. (a) is from an Al layer, buried 15 μm under the front surface and (b) from a Au layer at a depth of 50 μm. (c) is from a Au layer at a depth of 100 μm, viewed from the back of the foil. In contrast, (d) shows the solid spot emitted by a solid Au film [5] viewed from the front.

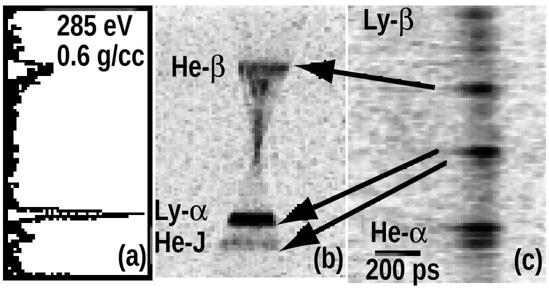

FIG. 2. (a) A fit, along with fitting parameters to (b) Mica spectrograph data from an Al layer 10 µm deep. (c) shows KAP spectrograph data from the same layer [5].

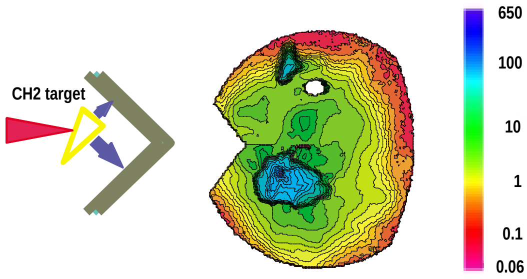

FIG. 3. Contours of dose in krads as a function of angle recorded on RC film through 300 µm Ta (proton E > 18 MeV). The image clearly shows two proton beams, the larger from the major face and the smaller from the minor face of the wedge [7].

for a Au target, it is ~ 40° for proton energies > 17 MeV narrowing to ~10° for energies > 30 MeV. The beams from metal targets, a cross-section that is nearly circular; it is much more irregular from CH targets. Observation of nuclear reactions gave direct evidence that the beam is protons rather than other ionic species. Deconvolution of the nuclear activation of a multilayer Be/Ti detector (interleaved with the radiochromic film) gave the absolute energy spectrum of the protons; it agreed well with values determined from radiochromic film density (Fig. 4). Details can be found in Snavely *et al.* [7].

Addition of a magnetic spectrometer also confirmed the proton's identity, and gave more details of the energy spectrum; the proton energy sharply cuts off at ~55 MeV for normal emission, and 15 MeV at 45°. Details can be found in Cowan *et al.* [8] and Roth *et al.* [9].

The source of the proton beam is well understood and attributable to electrostatic fields produced by hot electrons acting on protons at the rear surface (from adsorbed hydrocarbons for metal targets). These effects have been seen before [10]; During the Los Alamos Helios laser program, laser pulses with intensity×(wavelength)^2,Iλ^2, up to 10^{18} Wcm^{-2}µm^2 in ns pulses have produced proton energies up to a few MeV. The much more intense, shorter pulses used in these experiments (Iλ^2 ~ 10^{20} Wcm^{-2}µm^2 in a ps) created correspondingly more intense proton beams. This is modelled in detail by Wilks *et al.* [11]. He assumes laser creates very hot electrons (energy scaling with the ponderomotive potential of the laser) which expand into space on all sides of the sample. This creates an electric field at all surfaces whose magnitude depends on the ion density gradient at that surface. The laser prepulse creates a long-scale-length gradient on the front, minimizing acceleration in that direction), so almost all of the protons are accelerated from the front. Evidence of protons accelerated from corner edges and sides could be seen in some samples.

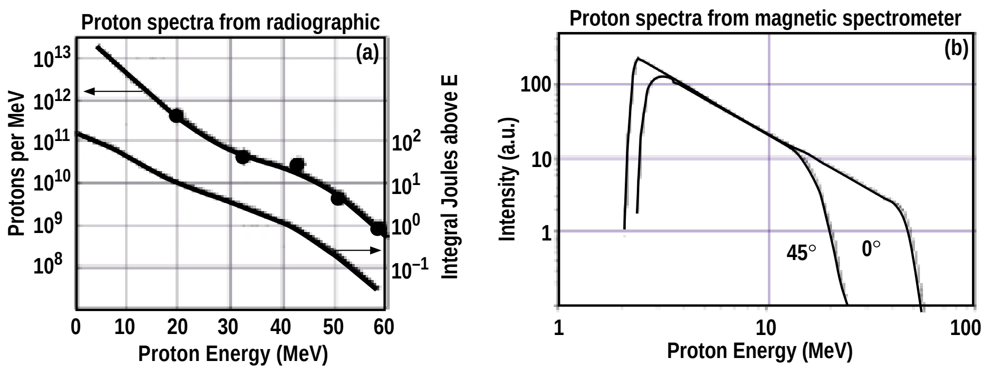

FIG. 4. (a) Proton energy spectrum deduced from radiochromic film images for a 423 J shot at normal incidence on 100 µm CH. (b) Spectrum of proton energy recorded on film with a magnetic deflection spectrometer. Plots show the spectrum on axis and from another shot at 45°. The detector is saturated above the cutoff region.

Using a proton beam can be advantageous for Fast Ignition. A focused ion beam may maintain an almost straight trajectory within the compressed target, and will deliver the energy in a well-defined volume due to the higher energy deposition at the end of its range. Roth *et al*. [9] have described a target configuration which would use protons to ignite a heavy-ion beam-compressed target (Fig. 5). They find that protons with an energy range 15-23 MeV could deposit their energy in a depth ~ 0.6 g/cm^3 with a time spread <10 ps added to the laser pulse length in a spot ~20 µm diameter. The efficiency with which this can be done will be critical in determining the utility of this approach, and is the subject of ongoing experiments.

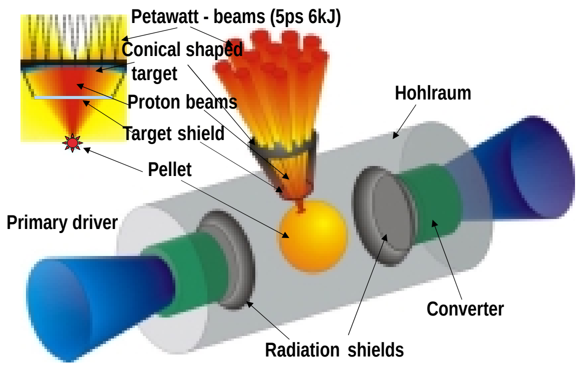

FIG. 5. Indirectly driven fast igntion using a laser accelerated proton beam (not to scale). The rear surface of the laser target is shaped to focus the ion beam into the spark volume.

4. Summary

Nova PW experiments have shown that electrons, which can be created with efficiency up to 50%, penetrate up to 200 µm deep into CH targets in a collimated fashion; this is substantially different from the ~90° spread in angles observed for electrons emitted from the back of the foil. Their passage heats the matrix to ~300 eV. The electron beam exhibits an annular structure which is not yet understood.

PW experiments have also shown proton beams as a possible alternative for delivering the ignition energy. The conversion efficiency is not so good to date (up to ~12% in these initial experiments), but the beams are tightly focussed, and have a spread of energies which is suitable for depositing the ignition energy in a small volume.

Acknowledgment

Work was supported by the U.S. Department of Energy by the Lawrence Livermore National Laboratory under contract No. W-7405-ENG-48, with the additional corporate support of General Atomics.

References

[1] KEY, M.H., et al., "Progress in fast ignitor research with the NOVA Petawatt Laser Facility," (Proc 17th Int. Conf. Yokohama, 1998) IAEA, Vienna (1999) (CD-ROM file IF/5).

[2] LASINSKI, B.F., LANGDON, A.B., HATCHETT, S.P., KEY, M.H, and TABAK, M., "Particle-in-cell Simulations of Ultra Intense Laser Pulses Propagating Through Overdense Plasma for Fast-Ignitor and Radiography Applications," Phys. Plasmas **6** 2041-2047 (1999).

[3] TALLENTS, G.J., KEY, M.H., NORREYS, P., BROWN, D., DUNN, J., BALDIS, H., "Production of Hot Near-Solid-Density Plasma by Electron Energy Transport in a Laser-Produced Plasma," Phys. Rev. A **40** 2857-2859 (1989); GUETHLEIN, G., FORD, M.E., and PRICE, D., "Electron Temperature Measurements of Solid Density Plasmas Produced by Intense Ultrashort Laser Pulses," Phys. Rev. Lett. **77** 1055-1058 (1996); KOCH, J.A. et al., Lasers and Particle Beams **16** 225 (1998).

[4] STEPHENS, R.B., KEY, M., KOCH, J., and PENNINGTON, D., "X-ray Imaging to Characterize MeV Electrons' Propagation Through Plastic Targets," Inertial fusion sciences and applications 99, ed. LABAUNE, C., HOGAN, W.J., AND TANAKA, K.A., (Elsevier, NYC, 2000), p. 480-483.

[5] KOCH, J., HATCHETT, S.P., KEY, M.H., LEE, R.W., PENNINGTON, D., STEPHENS, R.B., and TABAK, M., “Measurements of Deep Heating Generated By Ultra-Intense Laser-Lasma Interactions,” Inertial fusion sciences and applications 99, ed. LABAUNE, C., HOGAN, W.J., AND TANAKA, K.A., (Elsevier, NYC, 2000), p. 463-466; KOCH, J., HATCHETT, S.P., KEY, M.H., LEE, R.W., PENNINGTON, D., STEPHENS, R.B., and TABAK, M., “Observation Of Deep Directional Heating At Near-Solid Density Caused By Laser-Generated Relativistic Electrons,” submitted to PRL.

[6] KOCH, J.A., LANDEN, O.L., BARBEE, JR., T., BENNETT, G., BROWN, C., CELLIERS, P., COLLINS, G., Da SILVA, L., GLENDINNING, S., HAAN, S., HAMMEL, B., HSING, W., KALANTAR, D., KEY, M., SEELY, J., SUTER, L., WEBER, F., “Recent Progress in High-Energy, High-Resolution X-Ray Imaging Techniques for Application to the National Ignition Facility,” Rev. of Sci. Instrum. **70** 525-529 (1999).

[7] SNAVELY, R., KEY, M., HATCHETT, S., COWAN, T.E., ROTH, M., PHILLIPS, T.W., STOYER, M.A., HENRY, E.A., SANGSTER, T.C., SINGH, M.W., WILKS, S.C., MACKINNON,. A., OFFENBERGER, A., PENNINGTON, D.M., YASUIKE, K., LANGDON, A.B., LASINSKI, B.F., JOHNSON, J., PERRY, M.D., CAMPBELL, E.M., “Intense High Energy Proton Beams from Petawatt Laser Irradiation of Solids,” submitted To Phys. Rev. Lett. (1999).

[8] COWAN, T.E., Roth, M., JOHNSON, J., Le SAGE, G.P., HATCHETT, S.P., and WILKS, S.C., “Laser Generation of Accelerator Quality Proton Beams,” in: High Brightness Beams (World Scientific Press, Singapore, 2000), in press

[9] ROTH, M., COWAN, T.E., KEY, M., HATCHETT, S.P., BROWN, C., FOUNTAIN, W., JOHNSON, J., PENNINGTON, D.M., SNAVELY, R.A., WILKS, S.C., YASUIKE, K., RUHL, H., PEGORARO, P., BULANOV, S.V., POWELL, H., CAMPBELL, E.M., and PERRY, M.D., “Fast Ignition by Intense Laser-Accelerated Proton Beams,” submitted to Phys. Rev. Lett. (March, 2000).

[10] GITOMER, S.J., et al., Phys. Fluids **29** 2679 (1986).

[11] WILKS, S.C., LANGDON, A.B., COWAN, T.E., ROTH, M., SINGH, M., HATCHETT, S., KEY, M.H., PENNINGTON, D., MACKINNON, A., and SNAVELY, R.A., “Energetic Proton Generation in Ultra-Intense Laser-Solid Interactions,”to be published in Phys. Plasmas (2000).